PHYSICAL REVIEW E VOLUME 61, NUMBER 3 MARCH 2000

Switching dynamics in homeotropic ferroelectric liquid crystals

N. Pereda, C. L. Folcia, and J. Etxebarria
Departamento de Física de la Materia Condensada, Facultad de Ciencias, Universidad del País Vasco, Apartado 644, 48080 Bilbao, Spain

J. Ortega
Departamento de Física Aplicada II, Facultad de Ciencias, Universidad del País Vasco, Apartado 644, 48080 Bilbao, Spain

(Received 6 August 1999)

The molecular motion during the switching in homeotropic cells of chiral-smectic-*C* materials has been investigated by means of second-harmonic generation and electrooptic measurements. The analysis of the results shows that the director reorientation takes place within microdomains of size smaller than the optical wavelength. There are two types of domains which occur with different probabilities, and in each of them the molecules rotate in opposite directions. Moreover the optical indicatrix rotates in a preferential direction, which indicates that the dipole moments move from 0° to 360° during a whole switching period. This contrasts with the back and forth rotation from 0° to 180° observed in planar cells. The results are analyzed in view of the macroscopic symmetry of a chiral-smectic-*C* phase and a simple qualitative model is proposed which explains the observed behavior.

PACS number(s): 61.30.−v, 78.20.Jq, 42.65.Ky

I. INTRODUCTION

In the last years extensive attention has been given to the switching mechanisms of chiral smectic-*C* (Sm-*C**) ferroelectric liquid crystals (FLCs). Most of these studies have been made on planar cells because this geometry seems the most promising for device applications [1–10]. These investigations have shown that in general the cell surfaces have much influence on the molecular reorientation processes and the electro-optic response is complicated. In contrast, very few studies have been published on the behavior of homeotropic samples [11,12], where the molecules are virtually free of surface anchoring constraints. Recently, Drevensek Olenik *et al.* [13], on the basis of optical second harmonic generation (SHG) measurements, have shown that switching in homeotropic cells takes place in a rather peculiar manner. The director reorientation goes on within numerous microdomains of size much smaller than the visible wavelength. Two kinds of equally probable domains can be found, and in each of them the director rotates in opposite directions describing half a cone.

There is nothing similar to this behavior in the better known reorientation mechanisms of planar samples and, therefore, we have considered of interest to test the validity of this switching model. With this aim, we have performed SHG and electro-optic studies on two different FLC materials in homeotropic geometry. In our samples the measurements have ratified the main features of the model. Nevertheless, it has been found that a more complex process occurs in general, in the sense that the two types of domains have not the same probability. In addition, the electro-optic results indicate that at low frequencies the dipole moments of the molecules rotate from 0° to 360° during a whole switching period, in contrast to the behavior observed in planar samples.

II. SHG MEASUREMENTS

SHG measurements were carried out using a *Q*-switched Nd^{3+}:YAG laser operating at a wavelength $\lambda = 1064\,\mathrm{nm}$. The experimental setup has been described elsewhere [14]. A bipolar square-wave electric field was applied to the homeotropic sample in a direction parallel to the smectic planes. The laser pulse triggered an oscilloscope, where second harmonic (SH) light intensities were acquired, and was synchronized with the electric wave. The relative phase between the electric field at the sample and the trigger of the laser could be varied in steps of 0.01°, permitting therefore to measure the SH signal at different times during the switching process. This allowed us to achieve a time resolution of $\Delta t = 0.01/(360\nu)$, where ν is the frequency of the electric wave.

We will begin by showing our results for SCE9 (Merck), which was also the material studied in Ref. [13]. The material undergoes the following transitions: Sm-*C**–60 °C–Sm-*A*-89 °C–N*-115 °C-I. The measurements were made in the Sm-*C** phase at 25 °C where the material has a spontaneous polarization $P_S = 34\,\mathrm{nC/cm^2}$. The sample thickness was 50 μm. The frequency was $\nu = 5$ Hz and the amplitude of the field $E = 770$ V/mm, which is several times larger than the threshold field for helix unwinding. Figure 1 shows the time dependence of the angle of inci

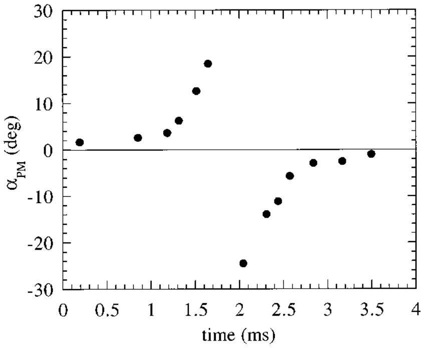

FIG. 1. Time dependence of α_{PM} during the switching. The time origin corresponds to the inversion of the square-wave electric field.

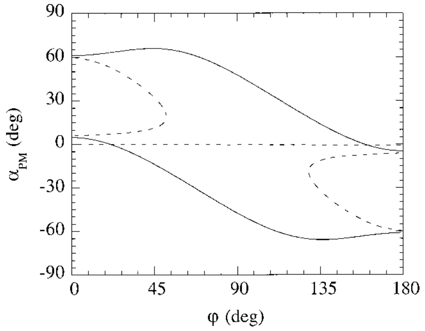

FIG. 2. Dependence of α_{PM} on the azimuthal angle φ of the director on the tilt cone. The continuous line corresponds to the microscopic multidomain model, according to which the molecules move on either side of the cone with probability $\frac{1}{2}$. The dashed line represents the case of a uniform process, where all the molecules move on the same side of the cone during the switching.

dence α_{PM} for which the phase matching (PM) condition is attained. This angle was determined by finding the maximal SH intensity as the sample was rotated about a (vertical) axis parallel to the electric field. During the whole experiment, the incident light was linearly polarized in the horizontal plane while SH light was detected after passing through a vertical analyzer. The conversion process is described as *ee-o* (two extraordinary waves combine to give one ordinary SH wave). The PM direction α_{PM} increases as the molecular reorientation starts. At the same time, SHG intensities begin to decrease, and after 1.7 ms no PM peak is visible. This situation is maintained during 0.3 ms approximately. Then the PM peak reappears but at opposite angles of incidence. Finally, the PM maxima grow again and their angular positions tend towards an incidence equal but opposite to the starting angle.

In Fig. 2 we have plotted the calculated α_{PM} on the phase angle φ of the director in the two switching models depicted in Fig. 3. Continuous line in Fig. 2 corresponds to Fig. 3(a), i.e., to the model described in Ref. [13]. Dashed line in Fig. 2 holds for the model according to which the molecules uniformly rotate on the tilt cone over the whole illuminated sample area [15] [Fig. 3(b)]. The optical parameters taken to draw Fig. 2 were the following. Ordinary and extraordinary indices at the fundamental wavelength $n_0(\omega)=1.52$, $n_e(\omega)=1.69$; material dispersion $n_o(2\omega)-n_o(\omega)=0.011$; molecular tilt angle $\theta=20.5°$.

As can be seen, results in Fig. 1 seem to fit better the uniform switching model Fig. 3(b) since during the reorientation α_{PM} does not cross the origin, in contrast with the data of Ref. [13]. In that work it was found that the PM angle passed twice through normal incidence in a whole switching period. However, care should be taken in interpreting these results. Unfortunately α_{PM} is close to zero near the extreme switching positions ($\varphi=0°$ and $\varphi=180°$) and there is an obvious experimental error. In addition, small changes in the material parameters give rise to predictions without any crossing through zero in either model (Fig. 4). Therefore, any conclusion in favor of one particular model seems premature in view of only these results.

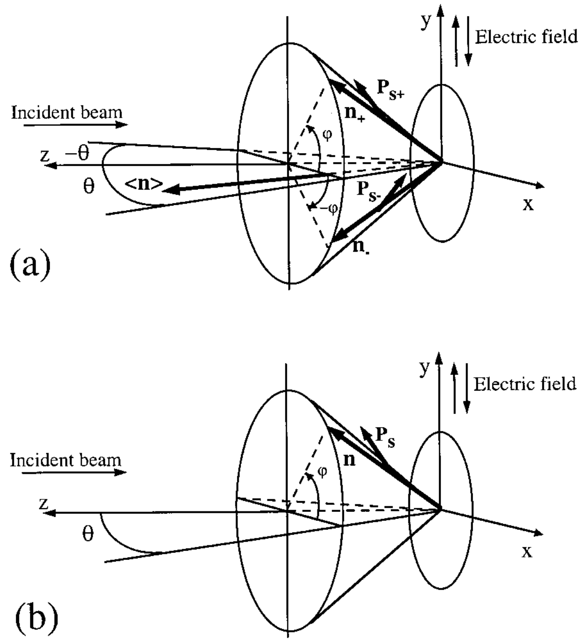

FIG. 3. Schematic representation of the director reorientation during the switching within the framework of a microscopic multidomain switching model (a) or a uniform model (b).

A second experimental point to be considered is the optical polarization of the SH beam. According to the results of Ref. [13], if the incident light is polarized in the horizontal plane the SH light is polarized in the vertical direction during the whole switching irrespective of the angle of incidence. This fact can only be understood within the framework of the multidomain switching model [Fig. 3(a)]. We have found however that there is actually a small component of the SH field polarized in the horizontal plane. In addition, we have detected transient SH light at normal incidence when the polarizer and analyzer are vertically and horizontally set, respectively (Fig. 5). It can be easily shown that there is no explanation for these features if the switching mechanism of Fig. 3(a) is assumed. Only if the average director $\langle \mathbf{n} \rangle$ in Fig. 3(a) deviates from the *xz* plane during the reorientation these two facts can be accounted for.

In view of these discrepancies we are led to propose a model hybrid between those in Figs. 3(a) and 3(b). It must be noted that our results do not mean that a macroscopic part of the sample reorients uniformly and the rest according to the multidomain model. If this were the case, SH intensities generated from both parts would add incoherently and two transient PM peaks (at angles of incidence roughly opposite) should have been observed in the measurements of Fig. 1

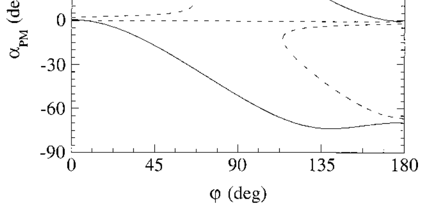

FIG. 4. The same representation as in Fig. 2, but considering slightly different optical parameters: $n_0(\omega)=1.53$, $n_e(\omega)=1.68$, $n_0(2\omega)-n_0(\omega)=0.012$, $\theta=20.5°$.

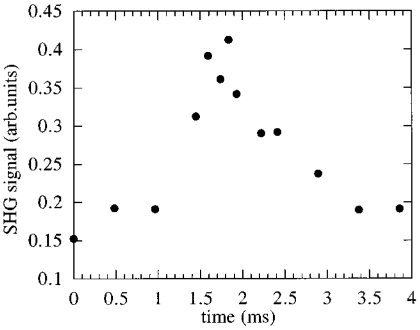

FIG. 5. Second harmonic intensity versus time for a homeotropic cell of SCE9 at normal incidence. The polarizer and analyzer were vertical and horizontal, respectively. The value of the maximum is to be compared with the size of the second harmonic signal in the usual *ee-o* configuration at normal incidence (≈5 in the same units).

(see continuous and dashed lines in Fig. 2 or Fig. 4). Instead, the data indicate that the actual mechanism is a coherent sum of the uniform and multidomain models. In other words, all the observations can be explained if there is an excess of microdomains of one particular type in the model of Fig. 3(a). In this situation, during the switching the projection of ⟨**n**⟩ on the smectic planes describes neither a circle nor a straight line but something in-between.

An approximate measure of the relative proportion of privileged domains can be obtained by comparing the magnitude of the peak in Fig. 5 with the SH intensity at normal incidence for the *ee-o* conversion when the sample is subjected to a dc field. Both intensities would be equal in the uniform model (in this case at $\varphi=90°$ both experimental geometries only differ in a rigid rotation of the set polarizer-sample-analyzer by 90°). On the other hand, as has been mentioned before, the signal in Fig. 5 would be zero if the two domains occurred with the same probability.

For SCE9 a ratio smaller than 1/10 has been obtained between both SH intensities at 25 °C, which means that the 50%:50% multidomain model of Fig. 3(a) works rather well for this material. Furthermore, this ratio tends to zero when we raise the temperature and approach the Sm-*C**–Sm-*A* transition. Figure 6 shows however a different situation. Now the material studied is W316 [16], which presents a phase sequence Sm-*C**-60 °C–Sm-*A*-90 °C-I, and is ferroelectric at room temperature. The data were taken at 25 °C and here the transient peak is much better defined and intense. In fact, the measurements practically agree with the 0%:100% uniform model (the above referred intensity ratio is higher than 0.85).

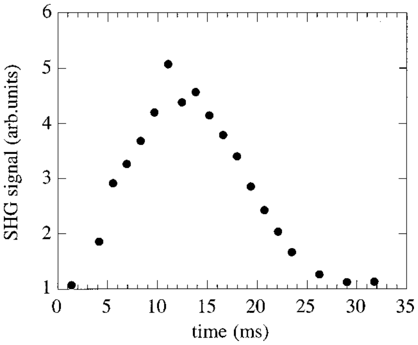

FIG. 6. Dependence of the second harmonic intensity on time for a homeotropic cell of W316 at normal incidence. The polarizer and analyzer were vertical and horizontal, respectively. The maximum of this curve is about 90% of the size of the second harmonic signal at normal incidence in the usual PM configuration (*ee-o*).

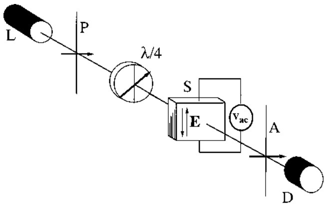

FIG. 7. Experimental setup for the electrooptic measurements. L = He-Ne laser, P = polarizer, $\lambda/4$ = quarter-wave plate, S = homeotropic sample, A = analyzer, D = photodiode, V_{ac} = square-wave function generator. The configuration shown corresponds to *M*2. For the *M*1 measurements the quarter wave plate is removed.

To summarize we can conclude that in general a hybrid model that combines the features of the schemes of Figs. 3(a) and 3(b) should be used. The amount of each type of domain depends on the particular material and temperature. An accurate numerical value for the relative proportion of each domain is difficult to be given by using only SHG measurements because too many material parameters are involved in the mathematical expressions. The problem will be addressed again in the next section within a simpler context.

III. ELECTRO-OPTIC MEASUREMENTS

In the light of the results obtained with the SHG measurements we have used a simpler method to complement the above conclusions and study more quantitatively the switching kinetics. The experimental setup is schematized in Fig. 7. The light from a stabilized He-Ne laser ($\lambda=632.8$ nm) passed sequentially through a polarizer, the sample and an analyzer, and was detected with a photodiode. The cell was homeotropically aligned and arranged at normal incidence. As before a square-wave electric field of 770 V/mm was applied to the sample along the vertical axis (y axis in Fig. 3). A frequency of 0.4 Hz was used, which was small enough to guarantee under visual inspection in the polarizing microscope that the two equilibrium states were attained during the switching. An oscilloscope was connected to the photodiode and to the function generator, so that both the transmitted light intensity and the electric wave could be scanned simultaneously in the oscilloscope as a function of time.

Two different experimental configurations were considered. In *M*1 both the polarizer and analyzer were fixed horizontally. In *M*2 a quarter-wave plate set at 45° with respect to the vertical axis was inserted between the polarizer and the sample in order to obtain circularly polarized light. During the reorientation process, the light transmitted in the two dispositions can be expressed as

$$I_1 \propto 1-\sin^2 2\alpha \sin^2\left(\frac{\pi \Delta n d}{\lambda}\right), \tag{1}$$

$$I_2 \propto 1+\sin 2\alpha \sin\left(\frac{2\pi \Delta n d}{\lambda}\right), \tag{2}$$

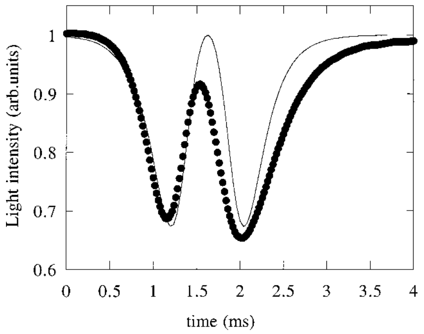

FIG. 8. Dependence of the transmitted intensity on time during the switching of a homeotropic cell of SCE9 in the $M1$ configuration. Circles are the experimental data and the continuous line represents the theoretical prediction assuming a 70%:30% multidomain model and a rotational viscosity $\gamma = 0.15\,\mathrm{Pa\,s}$.

respectively. Here α is the angle of the optical indicatrix projected on the xy plane and Δn the birefringence at normal incidence. In general, both α and Δn change during the switching, and their values depend on the amount of molecules going along either side of the cone. If we call x to the proportion of molecules switching on the upper side of the cone, it can be shown that $\Delta n = n_2 - n_1$ and α are given by

$$n_1^2 = n_0^2 + \frac{n_e^2 - n_0^2}{2} \times [1 - \sqrt{x^2 + (1-x)^2 + 2x(1-x)\cos 4\varphi}]\sin^2\theta, \quad (3)$$

$$n_2^2 = n_0^2 + \frac{n_e^2 - n_0^2}{2} \times [1 + \sqrt{x^2 + (1-x)^2 + 2x(1-x)\cos 4\varphi}]\sin^2\theta, \quad (4)$$

$$\alpha = \tan^{-1}\left[\frac{(2x-1)\sin 2\varphi}{\cos 2\varphi + \sqrt{x^2 + (1-x)^2 + 2x(1-x)\cos 4\varphi}}\right]. \quad (5)$$

It can be checked that if $x=1$ or $x=0$, the above equations yield the well-known results of the uniform switching model, whereas if $x=\frac{1}{2}$, expressions consistent with those of Ref. [13] are obtained. In this last case, α is always zero, and Eqs. (1) and (2) give time independent signals.

Figure 8 shows the experimental results corresponding to $M1$. The data refer to a $15\,\mu\mathrm{m}$ thick sample of SCE9 at 25 °C. A time varying signal can be clearly seen, in agreement with the SHG conclusions. Taking into account the relative size of the ac and dc intensities it is possible to calculate x. The best agreement is found for $x=0.7$, which corresponds to a 70%:30% multidomain model. The continuous line in Fig. 8 is the theoretical prediction under the assumption of a simple dynamic equation for the azimuthal angle

$$\gamma \frac{d\varphi(t)}{dt} = P_s E \sin\varphi(t), \quad (6)$$

where γ is the rotational viscosity of the material. A value $\gamma = 0.15\,\mathrm{Pa\,s}$ is obtained, in agreement with Ref. [13].

In Fig. 9 we have plotted I_2 after the inversion of the electric field in both directions. It can be seen that the signal behavior is the same independently of the switching direction which, according to Eq. (2), means that α increases monotonicaly with time. In other words, the optical indicatrix rotates in a definite sense during the switching. This behavior is rather unexpected because it means that the molecules describe a complete cone instead of the usual movement back and forth along half a cone as is observed in planar samples. If this were the case, the second signal in Fig. 9 would have appeared inverted respect to the first one. However, the invariance of I_2 on both switching directions was checked by focusing the laser beam on different points of the sample area and using different samples with thickness in the range 10–15 μm. The continuous line in Fig. 9 was calculated using Eqs. (2)–(5) with the x and γ values obtained previously.

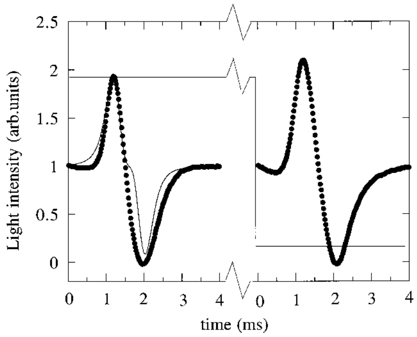

FIG. 9. Transmitted intensity versus time during the switching of a homeotropic cell of SCE9 in the $M2$ configuration. The two curves represent the signals after the − to + and + to − field inversions, respectively. The continuous line is the theoretical prediction.

Figures 10 and 11 show the time dependence of I_1 and I_2 for a 17 μm thick sample of W316 at 25 °C. Qualitatively the sample behaves similarly as SCE9. Here however the best fit gave $x=1$, so that in this case we have a pure uniform switching. Thus, in this material all the molecules rotate homogeneously describing a complete cone. The same dynamic equation (6) for $\varphi(t)$ was assumed and we got $\gamma = 3.4\,\mathrm{Pa\,s}$. The following material parameters were taken $P_S = 350\,\mathrm{nC/cm^2}$ [16], $n_e - n_o = 0.135$, and $\theta = 26°$ [14].

As can be seen the agreement can be considered satisfactory, although in all experimental curves (especially in Fig.

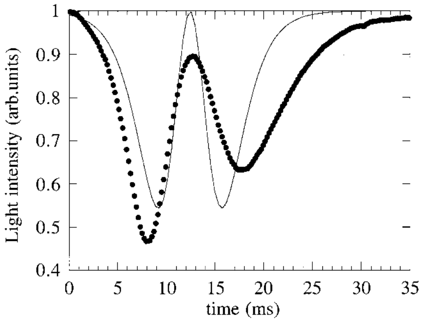

FIG. 10. Dependence of the transmitted intensity on time during the switching for a homeotropic cell of W316 in the $M1$ configuration. Circles are the experimental data and the continuous line corresponds to the prediction of a pure uniform switching model with $\gamma = 3.4\,\mathrm{Pa\,s}$.

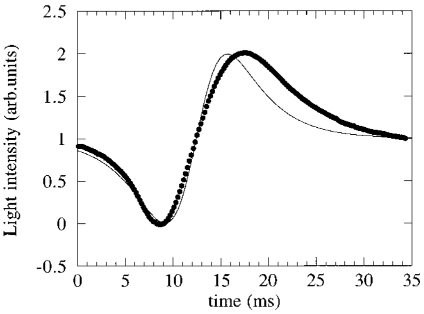

FIG. 11. Dependence of the transmitted intensity on time during the switching of a homeotropic cell of W316 in the *M*2 configuration. Circles are the experimental data and the continuous line corresponds to the prediction of a pure uniform switching model with $\gamma = 3.4$ Pa s.

10) the second part of the process seems to be systematically slower than the theoretical predictions. This probably indicates a slowing down of the molecular motion at the last part of the reorientation which cannot be explained by Eq. (6).

IV. DISCUSSION

Before attempting to explain the switching behavior observed in our cells, it is important to remark some aspects about the models represented in Fig. 3 in view of the macroscopic symmetry of an unwound Sm-C^* phase. First of all, it would be noted that the 50%:50% multidomain scheme is the only switching model in complete agreement with the existence of a twofold axis along $\mathbf{P}_S$, which prevents the macroscopic optical indicatrix to rotate in a particular direction. On the other hand, the uniform mechanism across the whole sample area is not compatible with the point group of the SmC* phase because there is no reason for the molecules to choose either half of the cone. It seems therefore that actually the symmetry of the cell is reduced in some way by the electric field, the cell surfaces being in last instance responsible of the phenomenon. This aspect of the problem was explicitly tested. We rotated one of our samples by 180° around the electric field direction and verified the obvious fact that the sense of rotation of the optical indicatrix is inverted (see Fig. 12). This simple experiment evidences the nonexistence of a twofold axis along **E**. Now the question is why the symmetry is reduced and what mechanism may be proposed for switching.

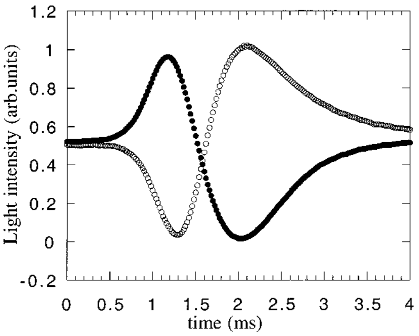

FIG. 12. Temporal dependence of the transmitted intensity during the switching of a homeotropic cell of SCE9 in the *M*2 configuration (full circles). The same signal after rotating the cell by 180° about an axis parallel to the electric field (open circles).

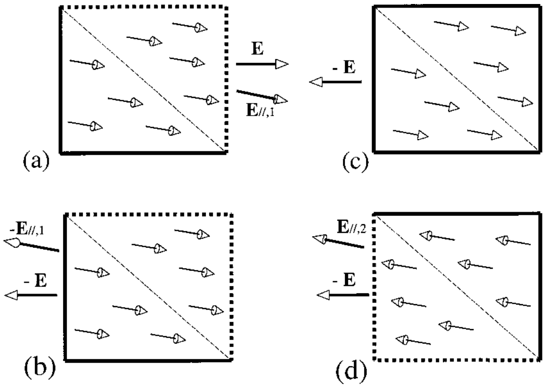

FIG. 13. Schematic representation proposed for the switching in homeotropic cells. A given smectic layer as viewed from the cell surface is shown. The layers are assumed to tilt about the diagonal dashed line. The arrows indicate the molecular dipole moments which are always rigidly contained in the layers. The electric field **E** and the initial and final in-plane components $\mathbf{E}_{\parallel,1}$, $\mathbf{E}_{\parallel,2}$ are also indicated. (a) Initial equilibrium situation. (b) The electric field has been inverted. (c) The layer tilt begins to reverse (a zero tilted layer is represented for simplicity), and the dipoles rotation starts (it is clockwise in the above scheme). (d) Final equilibrium situation.

In order to account for this, we will assume that a small tilt of the smectic layers induced by the electric field takes place in homeotropic cells. There are precedents of this phenomenon in planar cells with chevron structure, where small rotations of the smectic layers (about 1°) were observed by means of small angle x-ray diffraction experiments during the switching [17]. These results indicate that a fast rotation of the smectic layers occurs as the chevron angle is reduced by the electric field in order to conserve the number of layers. Our assumption is purely speculative since no experimental evidence exists about this phenomenon in homeotropic cells. Moreover, no estimation about the order of magnitude of the involved angles can be given, although it is likely that the system cannot depart significantly from the twofold symmetry.

Thus, the point group is reduced by the layers tilt. This rotation must proceed about a general direction not parallel to the electric field, and the tilt angle should reverse when the field is inverted. A very simple switching mechanism may be proposed now: The dipole moments (and therefore the macroscopic polarization) are contained in the smectic layers. These planes do not contain the electric field direction so that the dipoles are parallel to the in-plane component of **E**. No preferential switching direction appears when the electric field is suddenly inverted, i.e., the dipoles become antiparallel to the new in-plane **E** component. Nevertheless, when the layers tilt begins to reverse an azimuthal deviation of the dipoles in a given direction occurs (see Fig. 13). Furthermore, it can be easily seen that the dipoles always rotate in the same sense for both field inversions. The molecular rotation along the whole cone is thus explained.

The manifestation of the non uniform switching process in SCE9 can be attributed to a more widely extended statistical distribution of the directions of the dipoles at the switched states. This is in agreement with the lower $\mathbf{P}_S$ value of this material in comparison with W316. It could also be a consequence of a less effective mechanism for the layers rotation or some disorder in the parallelism of the smectic layers. To confirm the above hypothesis x-ray measurements of homeotropic samples under electric fields would be necessary. This work is being planned for the future.

ACKNOWLEDGMENTS

One of us (N.P.) is grateful to the Ministry of Education of Spain for a grant. This work was supported by the CICYT of Spain (Project No. MAT97-0986-02) and by the Universidad del País Vasco (Project No. 063.310-EB158/97).

[1] N. A. Clark and S. T. Lagerwall, Appl. Phys. Lett. **36**, 899 (1980).

[2] N. A. Clark, M. A. Handschy, and S. T. Lagerwall, Mol. Cryst. Liq. Cryst. **94**, 213 (1983).

[3] H. Orihara and Y. Ishibashi, Jpn. J. Appl. Phys. **23**, 1274 (1984).

[4] H. Takezoe, Y. Ouchi, K. Ishihawa, and A. Fukuda, Mol. Cryst. Liq. Cryst. **139**, 27 (1986).

[5] Y. Ouchi, H. Takezoe, and A. Fukuda, Jpn. J. Appl. Phys. **26**, 1 (1987).

[6] Y. Ouchi, H. Takano, H. Takezoe, and A. Fukuda, Jpn. J. Appl. Phys. **26**, L21 (1987).

[7] W. Hartmann, Ferroelectrics **85**, 455 (1988).

[8] L. A. Beresnev and L. M. Blinov, Ferroelectrics **92**, 729 (1989).

[9] J. W. Goodby, R. Blinc, N. A. Clark, S. T. Lagerwall, M. A. Osipov, S. A. Pikin, T. Sakurai, K. Yoshino, and B. Zeks, *Ferroelectric Liquid Crystals: Principles, Properties and Applications*, Vol. 7 of *Ferroelectricity and Related Phenomena*, edited by G. W. Taylor (Gordon and Breach, Philadelphia, 1991).

[10] B. Park, M. Nakata, S. S. Seomun, Y. Takanishi, K. Ishikawa, and H. Takezoe, Phys. Rev. E **59**, R3815 (1999).

[11] M. Ozaki and K. Yoshino, Jpn. J. Appl. Phys. **28**, L1830 (1989).

[12] I. Drevensek, R. Torre, and M. Copic, Mol. Cryst. Liq. Cryst. **251**, 101 (1994).

[13] I. Drevensek Olenik, R. Torre, and M. Copic, Phys. Rev. E **50**, 3766 (1994).

[14] N. Pereda, C. L. Folcia, J. Etxebarria, J. Ortega, and M. B. Ros, Liq. Cryst. **24**, 451 (1998).

[15] X. Jiu-Zhi, M. A. Handschy, and N. A. Clark, Ferroelectrics **73**, 305 (1987).

[16] D. M. Walba, M. B. Ros, N. A. Clark, R. Shao, K. M. Johnson, M. G. Robinson, J. Y. Liu, and D. J. Doroski, Mol. Cryst. Liq. Cryst. **198**, 51 (1991).

[17] H. F. Gleeson and A. S. Morse, Liq. Cryst. **21**, 755 (1996).